International Journal of Mass Spectrometry 309 (2012) 63–69

Contents lists available at SciVerse ScienceDirect

International Journal of Mass Spectrometry

journal homepage: www.elsevier.com/locate/ijms

A new impulsional potential for a Paul ion trap

S. Seddighi Chaharborj[a,b,*], S.M. Sadat Kiai[c], M.R. Abu Bakar[a], I. Ziaeian[c], I. Fudziah[a]

[a] Department of Mathematics, Faculty of Science, Universiti Putra Malaysia, 43400 UPM, Serdan-Selangor, Malaysia
[b] Islamic Azad University, Science and Research Branch, Department of Mathematics, Bushehr, Iran
[c] Physics Department, Nuclear Science Research School, Nuclear Science and Technology Research Institute (NSTRI), P.O. Box 14395-836, Tehran, Iran

ARTICLE INFO

Article history:
Received 16 March 2011
Received in revised form 27 August 2011
Accepted 27 August 2011
Available online 23 September 2011

Keywords:
Ion
Confinement
Paul ion trap
Impulsional potential
Fifth-order Runge–Kutta method
Mass separation

ABSTRACT

The dynamical behavior of an ion confined in a Paul ion trap supplied with a new periodic impulsional potential in the form as $f(t) = V((\cos \Omega t \lfloor 1 + k \cos 2\Omega t \rfloor)/(1-k))$; $0 \le k < 1$ ($\lfloor \cdot \rfloor$ means floor function) is considered and eventually compared to the classical sinusoidal case, $k = 0$. The new potential presents large zero potential temporal zones and the numerical integration of the Mathieu equation with the help of the fifth-order Runge–Kutta method showed some reduction in the stability diagrams, but for the same β, the properties of the confined ions stayed the same. Also, for given operational parameters such as $\Omega = 2\Pi \times 1.05 \times 10^6$ rad s^{-1}, $z_0 = 0.783$ cm, and *rf* only mode $U = 0$ ($a_z = 0$), the potential difference V_{rf} values for $m = 1$ and $m = 2$ ions is found to be $V_{rf} = 11$ V for $k = 0$ and $V_{rf} = 130$ V for $k = 0.9$. A larger separation, about 12 times for the impusional voltage compared to the classical sinusoidal which in term means a better mass separations and detection.

1. Introduction

The confinement of gaseous ions in a Mathieu's first stability region of a radio-frequency linear quadrupole ion trap; two dimensional confinement, or in a Paul ion trap or quadrupole ion trap (QIT); three dimensional confinement, is a well known process and is extensively used in wide variety of experiments and applications [1–3,5–13]. While, QIT functioning as an ion source or a mass spectrometer, generally, the device employs classical sinusoidal potential form. In the past, with the aim of injecting particle from outside into trap and increasing the voltage separations of different confined masses, a periodic impulsional voltage of the form $f(t) = V((\cos \Omega t)/(1 - k \cos 2\Omega t))$; $0 \le k < 1$ was constructed and used [11,14–19,21]. The subject of the present study is devoted to a general survey of a QIT behavior under the new periodic impusional voltage of the form $f(t) = V((\cos \Omega t \lfloor 1 + k \cos 2\Omega t \rfloor)/(1-k))$; $0 \le k < 1$. The new potential, for a given k's value, has a larger zero potential temporal zones and the first stability diagram compared to the pervious impulsional voltage form [14–19]. The numerical integration of the Mathieu equation with the help of the fifth-order Runge–Kutta method is explained and the fifth stability diagrams are studied and compared to the classical sinusoidal. Also, the first Mathieu's stability regions, the ion trajectories both in real time, $r-z$ plane and phase space, and QIT in *rf* only mode ($a_z = 0$) are discussed and presented.

2. Runge–Kutta method

To find the stability diagram's with high accuracy we have used the higher order Runge–Kutta method (improvements fifth order Runge–Kutta method) [20] as follows,

$$y_{n+1} = y_n + h(b_1k_1 + b_2k_2 + b_3k_3 + b_4k_4 + b_5k_5),$$

with

$$\begin{aligned}
k_1 &= f(x_n, y_n),\\
k_2 &= f(x_n + ha_2, y_n + ha_2k_1),\\
k_3 &= f\left(x_n + ha_3, y_n + ha_3\frac{k_1 + k_2}{2}\right),\\
k_4 &= f\left(x_n + ha_4, y_n + ha_4\frac{k_1 + k_2 + k_3}{3}\right),\\
k_5 &= f\left(x_n + ha_5, y_n + ha_5\frac{k_1 + k_2 + k_3 + k_4}{3}\right),
\end{aligned}$$

b_1, b_2, b_3, b_4 and b_5 are the weights chosen so that the parameters a_2, a_3, a_4 and a_5 can be determined and $(1/n)\sum_{i=1}^{n} k_i$ is defined as the arithmetic mean. For simplicity of the algebra, we consider f

* Corresponding author. Tel.: +60 389437958; fax: +60 389437958.
E-mail addresses: sarkhosh@math.upm.edu.my, sseddighi2007@yahoo.com (S.S. Chaharborj).

1387-3806/$ – see front matter © 2011 Elsevier B.V. All rights reserved.
doi:10.1016/j.ijms.2011.08.027

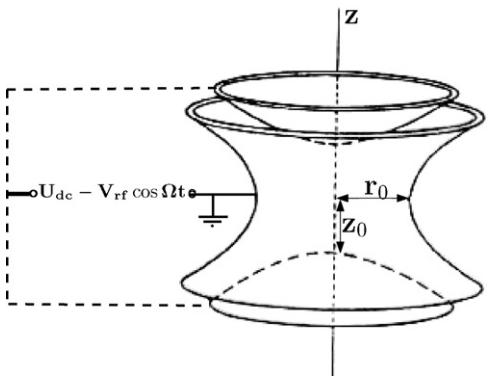

Fig. 1. Schematic view of a quadrupole ion trap.

as a function of y, without loss of generality. This will reduce the Taylor series expansion of k_i, $i = 1, 2, 3, 4, 5$ to the following,

$$
\begin{aligned}
k_1 &= f,\\
k_2 &= f + fha_2 f_y + \frac{1}{2} f^2 h^2 a_2^2 f_{yy},\\
k_3 &= f + \frac{1}{2} ha_3 f_y \left(2f + fha_2 f_y + \frac{1}{2} f^2 h^2 a_2^2 f_{yy}\right)\\
&\quad + \frac{1}{8} h^2 a_3^2 f_{yy} \left(2f + fha_2 f_y + \frac{1}{2} f^2 h^2 a_2^2 f_{yy}\right)^2,\\
k_4 &= f + \frac{1}{3} ha_4 f_y \left(3f + fha_2 f_y + \frac{1}{2} f^2 h^2 a_2^2 f_{yy}\right)\\
&\quad + \frac{1}{2} ha_3 f_y \left(2f + fha_2 f_y + \frac{1}{2} f^2 h^2 a_2^2 f_{yy}\right)\\
&\quad + \frac{1}{8} h^2 a_3^2 f_{yy} \left(2f + fha_2 f_y + \frac{1}{2} f^2 h^2 a_2^2 f_{yy}\right)^2,\\
k_5 &= f + \frac{1}{4} ha_5 f_y \left(4f + fha_2 f_y + \frac{1}{2} f^2 h^2 a_2^2 f_{yy}\right)\\
&\quad + \frac{1}{2} ha_3 f_y \left(2f + fha_2 f_y + \frac{1}{2} f^2 h^2 a_2^2 f_{yy}\right)\\
&\quad + \frac{1}{8} h^2 a_3^2 f_{yy} \left(2f + fha_2 f_y + \frac{1}{2} f^2 h^2 a_2^2 f_{yy}\right)^2\\
&\quad + \frac{1}{3} ha_4 f_y \left(3f + fha_2 f_y + \frac{1}{2} f^2 h^2 a_2^2 f_{yy}\right)\\
&\quad + \frac{1}{2} ha_3 f_y \left(2f + fha_2 f_y + \frac{1}{2} f^2 h^2 a_2^2 f_{yy}\right)\\
&\quad + \frac{1}{8} h^2 a_3^2 f_{yy} \left(2f + fha_2 f_y + \frac{1}{2} f^2 h^2 a_2^2 f_{yy}\right)^2\\
&\quad + \frac{1}{18} h^2 a_3^2 f_{yy} \left(3f + fha_2 f_y + \frac{1}{2} f^2 h^2 a_2^2 f_{yy}\right)\\
&\quad + \frac{1}{2} ha_3 f_y \left(2f + fha_2 f_y + \frac{1}{2} f^2 h^2 a_2^2 f_{yy}\right),
\end{aligned}
$$

with, $b_1 = -3.7783286500685627$, $b_2 = -0.18312885616492072$, $b_3 = 0.04837565197099888$, $b_4 = -17.700904612988186$, $b_5 = 22.61398646725067$, $a_2 = 0.6826487126671337$, $a_3 = 2.7638749083367884$, $a_4 = 0.1$, and $a_5 = 0.1$.

3. Study the motions of ion voltage inside QIT

Fig. 1 shows a schematic view of a quadrupole ion trap (QIT). The QIT is the ion trap with hyperbolic geometry and is composed of a ring and two end cap electrodes facing each other in the z-axis. z_0 is the distance from the center of the QIT to the end cap and r_0 is the distance from the center of the QIT to the nearest ring surface. The easiest way to trap a charge particles, is to force the particles to vibrate and swing in limited space. This force present as,

$$F = -kR, \tag{1}$$

where R is the distance from the center of swing and k is constant. This force causes the oscillating particle to move around the equilibrium point will be caused by a parabolic potential as follows,

$$\Phi = -\int F \cdot dR = \frac{1}{2} kR^2 = \frac{1}{2} k(r^2 + z^2), \tag{2}$$

here $R^2 = r^2 + z^2$, $r^2 = x^2 + y^2$ and x, y, z are the Cartesian space components. Any potential in free space, should satisfy the Laplace equation as,

$$\nabla^2 \Phi = 0. \tag{3}$$

So that we see Eq. (2) cannot satisfy in the Laplace condition. So, to trap the ions in two dimensions we need to take complex potential as follows,

$$\Phi(x, y, z) = A(\alpha x^2 + \beta y^2 + \gamma z^2), \tag{4}$$

to satisfy Eq. (4), in Laplace condition, $\nabla^2 \Phi = 0$, we assume, $\alpha = \beta = 1$, $\gamma = -2$. Therefore,

$$\Phi(x, y, z) = A(x^2 + y^2 - 2z^2) = A(r^2 - 2z^2). \tag{5}$$

This potential can be produced by four hyperbolic electrodes. To obtain this form of electrodes, we can consider the surfaces with same potential $\Phi_0/2$ and $-\Phi_0/2$, as follows,

$$\Phi(r_0, 0) = \Phi_0/2 \quad and \quad \Phi(0, z_0) = -\Phi_0/2. \tag{6}$$

With this conditions we can find, $A = (\Phi_0)/(2r_0^2)$ and $A = (\Phi_0)/(4z_0^2)$, so $r_0^2 = 2z_0^2$. Thus, electrodes shape for the potential (4) are as,

$$\Phi = \frac{\Phi_0}{2r_0^2}(r^2 - 2z^2) = \pm 1, \tag{7}$$

Eq. (7) presents a hyperbolic equations for this potential. The potential Φ_0 is applied to the hyperbolic rod's can be written as,

$$\Phi_0 = U_{dc} - V_{rf} \frac{\cos \Omega t \lfloor 1 + k \cos 2\Omega t \rfloor}{1 - k} \quad with \quad 0 \le k < 1. \tag{8}$$

And for the potential Φ, we have,

$$\Phi = \frac{\Phi_0}{2r_0^2}(r^2 - 2z^2) = \frac{1}{2r_0^2}(r^2 - 2z^2)\left(U_{dc} - V_{rf} \frac{\cos \Omega t \lfloor 1 + k \cos 2\Omega t \rfloor}{1 - k}\right). \tag{9}$$

The electric field components in the trap become,

$$(E_r, E_z) = E = -\nabla \Phi(r, z), \tag{10}$$

where ∇ is gradient. From Eq. (10) we have,

$$(E_r, E_z) = \begin{bmatrix} -\dfrac{U_{dc} - (V_{rf}(\cos \Omega t \lfloor 1 + k \cos 2\Omega t \rfloor)/(1 - k))}{r_0^2} r \\ \dfrac{U_{dc} - (V_{rf}(\cos \Omega t \lfloor 1 + k \cos 2\Omega t \rfloor)/(1 - k))}{r_0^2} 2z \end{bmatrix}, \tag{11}$$

therefore,

$$E_r = -\frac{U_{dc} - (V_{rf}(\cos \Omega t \lfloor 1 + k \cos 2\Omega t \rfloor)/(1 - k))}{r_0^2} r, \tag{12}$$

$$E_z = \frac{U_{dc} - (V_{rf}(\cos \Omega t \lfloor 1 + k \cos 2\Omega t \rfloor)/(1 - k))}{r_0^2} 2z. \tag{13}$$

The equations of motion for a singly charged positive ion in the QIT are given by,

$$\frac{d^2 z}{d\tau^2} + \left(a_z - 2q_z \frac{\cos 2\tau \lfloor 1 + k \cos 4\tau \rfloor}{1 - k}\right) z = 0, \tag{14}$$

$$\frac{d^2 r}{d\tau^2} + \left(a_r - 2q_r \frac{\cos 2\tau \lfloor 1 + k \cos 4\tau \rfloor}{1 - k}\right) r = 0. \tag{15}$$

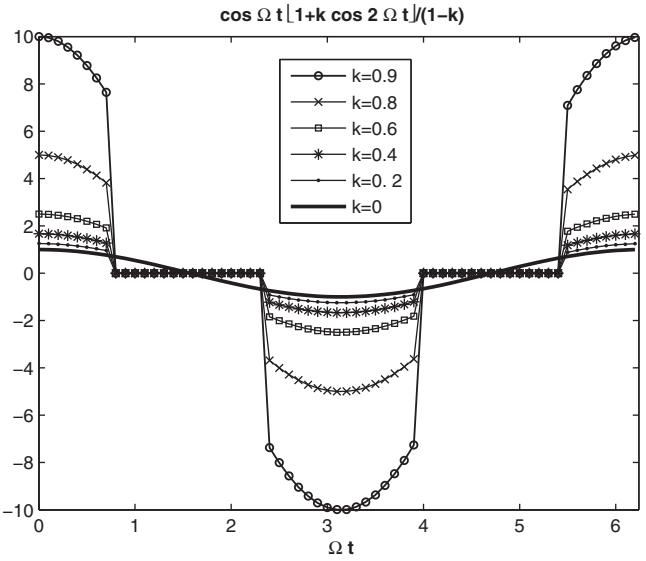

Fig. 2. Shape of potential function for impulsional potentials of the form $(\cos \Omega t \lfloor 1 + k \cos 2\Omega t \rfloor)/(1-k)$ for $0 \leq k < 1$.

The a and q parameters for z and r components as well as the dimensionless parameter τ are defined as follows,

$$\tau = \frac{\Omega t}{2}, \quad a_z = -2a_r = -\frac{4eU_{dc}}{mz_0^2\Omega^2}, \quad q_z = -2q_r = \frac{2(1-k)eV_{rf}}{mz_0^2\Omega^2}, \tag{16}$$

where m is the ion mass and e is the electronic charge. Now, for $k = 0$ we have,

$$\frac{d^2z}{d\tau^2} + (a_z - 2q_z \cos 2\tau)z = 0, \tag{17}$$

$$\frac{d^2r}{d\tau^2} + (a_r - 2q_r \cos 2\tau)r = 0. \tag{18}$$

with,

$$\tau = \frac{\Omega t}{2}, \quad a_z = -2a_r = -\frac{4eU_{dc}}{mz_0^2\Omega^2}, \quad q_z = -2q_r = \frac{2eV_{rf}}{mz_0^2\Omega^2}. \tag{19}$$

Fig. 2 shows the comparison of periodic impulsional potential of the form $V_{rf}((\cos \Omega t \lfloor 1 + k \cos 2\Omega t \rfloor)/(1-k))$, presented in this paper when $k = 0 ; 0.2 ; 0.4 ; 0.6 ; 0.8 ; 0.9$.

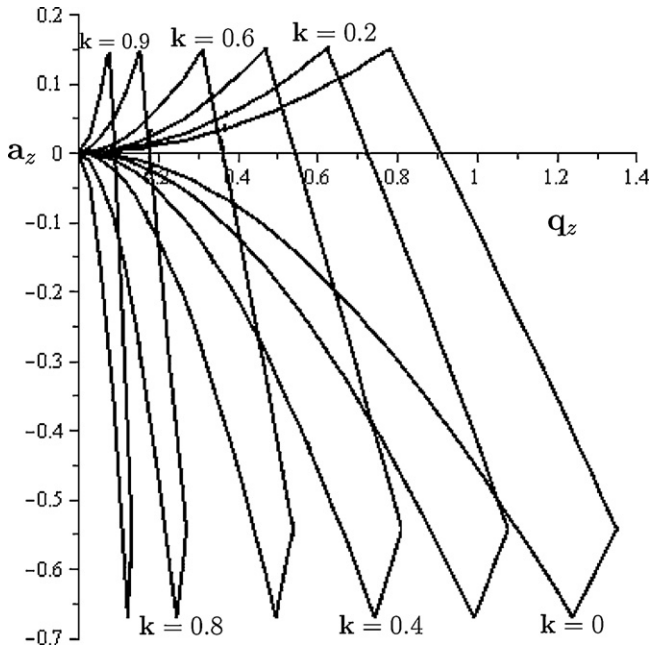

Fig. 3. The first stability region or the QIT with $k = 0 ; 0.2 ; 0.4 ; 0.6 ; 0.8 ; 0.9$.

4. Results

4.1. Stability regions

There are two stability parameters which control ion motion for each dimension u ($u = z$ or $u = r$); a_u, q_u in the case of quadrupole ion trap. In the plane (a_u, q_u) for the axis z, the ion stable and unstable motions are determine by comparing the amplitude of the movement to one for various values of a_z, q_z.

To compute the accurate elements of the motion equations for the stability diagrams, a fifth order Runge–Kutta method is employed. Fig. 3 presents the calculated first stability region with $k = 0 ; 0.2 ; 0.4 ; 0.6 ; 0.8 ; 0.9$ and Fig. 4(a) and (b) presents the calculated second stability region with $k = 0$ and $k = 0.9$ for the quadrupole ion trap using 0.001 steps ($h = 0.001$) increment in fifth order Runge–Kutta method. Figs. 3 and 4 show when k increase from 0 to 0.9 then the apex of the stability parameters a_z stayed the same and the apex of the stability parameters q_z decrease.

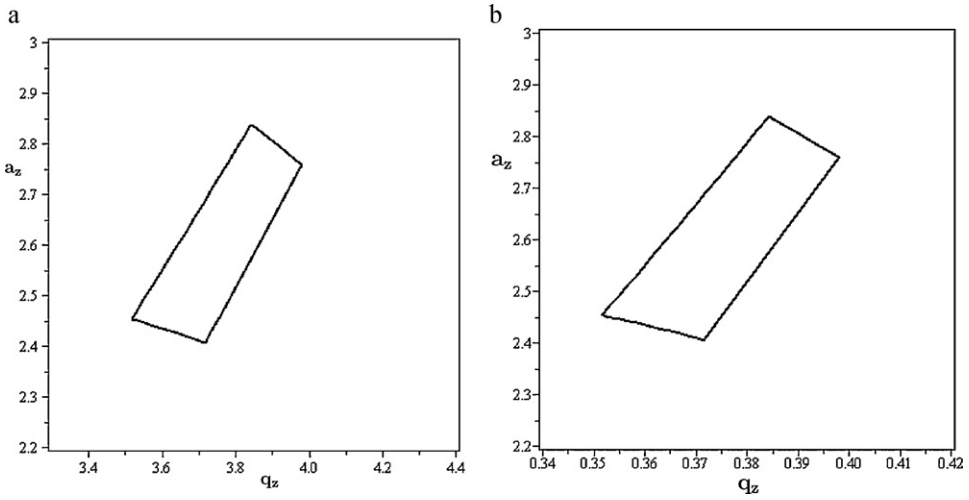

Fig. 4. The second stability region for the QIT, (a): $k = 0$ and (b): $k = 0.9$.

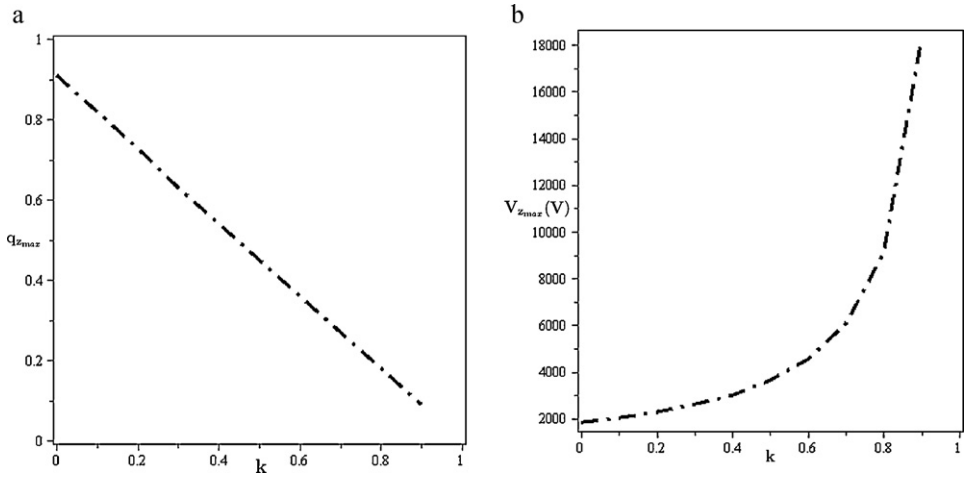

Fig. 5. (*a*): q_{zmax} as a function of k in a QIT defined for first stability region when $0 \le k < 1$ and $a_z = 0$, (*b*): V_{zmax} as a function of k for ^{131}Xe with $\Omega = 2\Pi \times 1.05 \times 10^6$ rad/s, $U = U_{dc} = 0$ V, $z_0 = 0.783$ cm in a QIT defined for first stability region when $0 \le k < 1$ and $a_z = 0$.

In Fig. 3, the first stability diagram is represented by $a_0, b_1, -2a_0, -2b_1$ and in Fig. 4, the second stability diagram is represented by $a_1, b_2, -2a_0, -2b_1$. Here, a_0, a_1, b_1, b_2 are as follows [4],

$$a_0 = -1/2\,\frac{q^2}{(1-k)^2} + \frac{7}{128}\,\frac{q^4}{(1-k)^4} - \frac{29}{2304}\,\frac{q^6}{(-1+k)^6} + \cdots, \tag{20}$$

$$a_1 = 1 + \frac{q}{1-k} - \frac{1}{8}\,\frac{q^2}{(1-k)^2} - \frac{1}{64}\,\frac{q^3}{(1-k)^3} - \frac{1}{1536}\,\frac{q^4}{(1-k)^4} \frac{11}{36,864}\,\frac{q^5}{(1-k)^5} + \frac{49}{589,824}\,\frac{q^6}{(1-k)^6} + \frac{55}{9,437,184}\,\frac{q^7}{(1-k)^7} + \cdots, \tag{21}$$

$$b_1 = 1 - \frac{q}{1-k} - \frac{1}{8}\,\frac{q^2}{(1-k)^2} + \frac{1}{64}\,\frac{q^3}{(1-k)^3} - \frac{1}{1536}\,\frac{q^4}{(1-k)^4} - \frac{11}{36,864}\,\frac{q^5}{(1-k)^5} + \frac{49}{589,824}\,\frac{q^6}{(1-k)^6} - \frac{55}{9,437,184}\,\frac{q^7}{(1-k)^7} + \cdots, \tag{22}$$

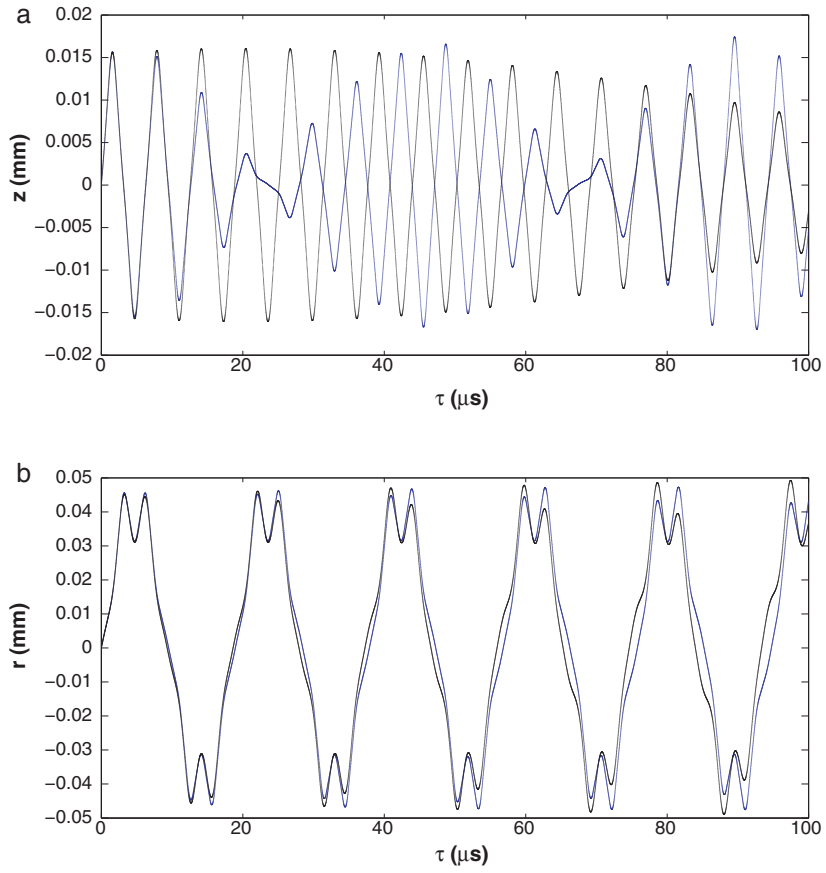

Fig. 6. The ion trajectories in real time for $\beta_z = 0.99$, black line: $k = 0$ and blue line: $k = 0.9$. (For interpretation of the references to color in this figure legend, the reader is referred to the web version of the article.)

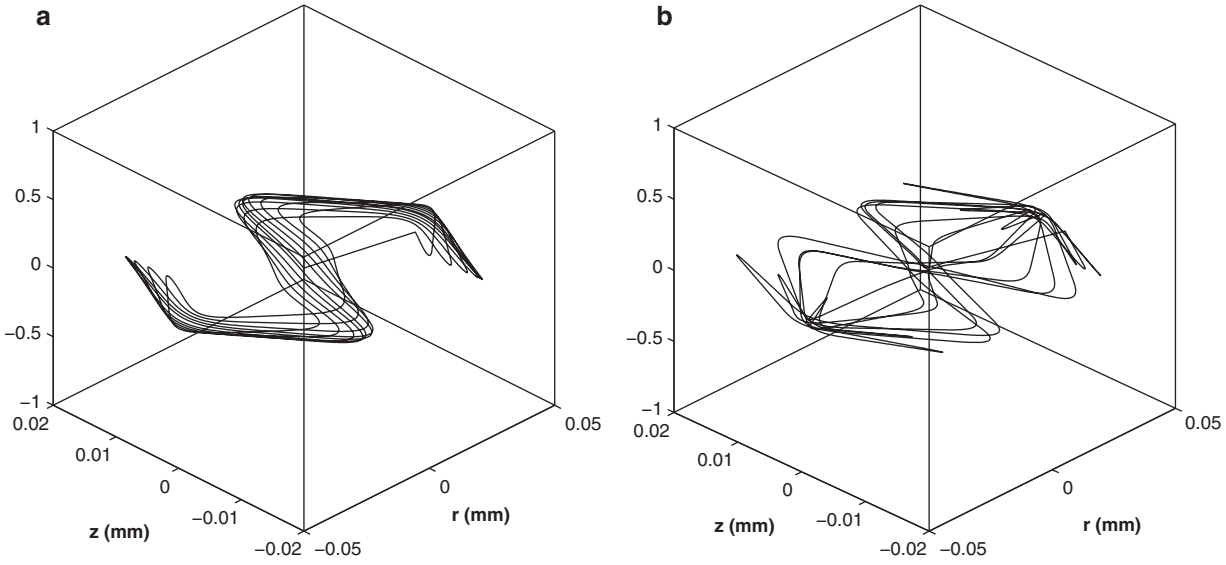

Fig. 7. The ion trajectory in $r-z$ plan for $\beta_z = 0.99$, (a) $k = 0$ and (b) $k = 0.9$.

$$b_2 = 4 - \frac{1}{12}\frac{q^2}{(1-k)^2} + \frac{5}{138,24}\frac{q^4}{(1-k)^4} + \frac{289}{79,626,240}\frac{q^6}{(1-k)^6} + \ldots, \quad (23)$$

Table 1 shows the values of (a_z, q_z) at the lower and upper tips for the first stability region of a QIT when $k = 0\,;0.9$. In other words, coordinates (a_z, q_z) with minimum and maximum a_z. To obtain Table 1 values we used the Eqs. (20) and (22). Table 1 values shows the intersection points of $-2a_0$ with b_1 and a_0 with $-2b_1$ when $k = 0\,;0.9$.

Table 1
The values of (a_z, q_z) at the lower and upper tips for the first stability region of a QIT when $k = 0\,;0.9$ (coordinates (a_z, q_z) with minimum and maximum a_z for $k = 0\,;0.9$).

k	(a_z, q_z)	
	Lower tip	Upper tip
0.0	(−0.67, 1.25)	(0.15, 0.78)
0.9	(−0.67, 0.12)	(0.15, 0.08)

Table 2
The values of $q_{z_{max}}$ when $a_z = 0$ for the quadrupole ion trap in the first stability region when $k = 0\,;0.2\,;0.4\,;0.6\,;0.8\,;0.9$.

k	0.0	0.2	0.4	0.6	0.8	0.9
$q_{z_{max}}$	0.91	0.72	0.54	0.36	0.18	0.09

Table 2 is the values of $q_{z_{max}}$ for the quadrupole ion trap in the first stability region when $k = 0\,;0.2\,;0.4\,;0.6\,;0.8\,;0.9$ for $a_z = 0$. To obtain this values we find the answers of the equation $b_1 = 0$ when $k = 0\,;0.2\,;0.4\,;0.6\,;0.8\,;0.9$.

Table 3 shows the values of $V_{z_{max}}$ for ^{131}Xe with $\Omega = 2\Pi \times 1.05 \times 10^6$ rad/s, $U = U_{dc} = 0$ V, $z_0 = 0.783$ cm and $a_z = 0$ in the first stability region when $k = 0\,;0.2\,;0.4\,;0.6\,;0.8\,;0.9$. To obtain the values of Table 3 we used the following relationship,

$$V_{z_{max}} = \frac{mz_0^2\Omega^2 q_{z_{max}}}{2e(1-k)}. \quad (24)$$

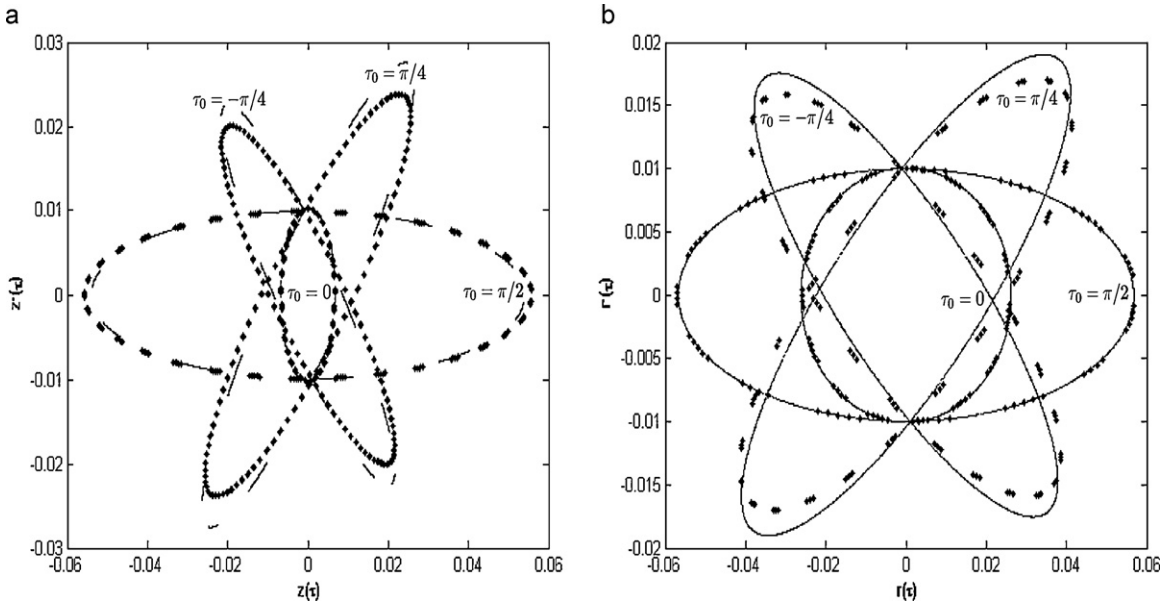

Fig. 8. The evolution of the phase space ion trajectory for different values of the phase τ_0 for $\beta_z = 0.99$, line: $k = 0$, dot line: $k = 0.9$, (a) $z - \dot{z}$ plan and (b) $r - \dot{r}$ plan.

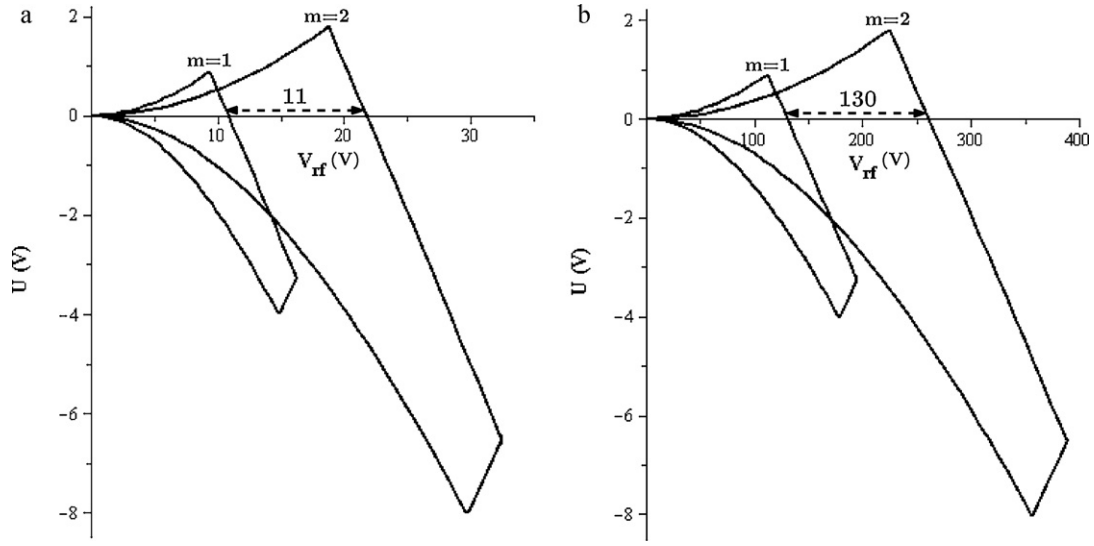

Fig. 9. The stability diagram in (U, V) for $m = 1$ amu, $m = 2$ amu, $\Omega = 2\Pi \times 1.05 \times 10^6$ rad/s, $z_0 = 0.783$ cm and (a) $k = 0$, and (b) $k = 0.9$.

Table 3
The values of $V_{z_{max}}$ when $a_z = 0$ for ^{131}Xe with $\Omega = 2\Pi \times 1.05 \times 10^6$ rad/s, $U = U_{dc} = 0$ V, $z_0 = 0.783$ cm in the first stability region when $k = 0\,; 0.2\,; 0.4\,; 0.6\,; 0.8\,; 0.9$.

k	0.0	0.2	0.4	0.6	0.8	0.9
$V_{z_{max}}(V)$	1812	2265	3020	4529	9059	18,118

Here $q_{z_{max}}$ is second row values of Table 2. To find the values of Table 3, we suppose $V_{z_{max}}$ as function of m, z_0^2, Ω^2, e and $(1-k)$ as follows,

$$V_{z_{max}} \propto \frac{mz_0^2\Omega^2}{2e(1-k)}. \tag{25}$$

Now, we use Eq. (25) to calculate $V_{z_{max}}$ for ^{131}Xe with $\Omega = 2\Pi \times 1.05 \times 10^6$ rad/s and $z_0 = 0.783$ cm when $k = 0\,; 0.9$ as follows,

$$V_{z_{max}} = \frac{(131/(6.022 \times 10^{26}))^2 \times (0.783 \times 10^{-2})^2 \times (2\pi \times 1.05 \times 10^6)^2}{2 \times 1.602 \times 10^{-19} \times (1-0)} \simeq 1812,$$

$$V_{z_{max}} = \frac{(131/(6.022 \times 10^{26}))^2 \times (0.783 \times 10^{-2})^2 \times (2\pi \times 1.05 \times 10^6)^2}{2 \times 1.602 \times 10^{-19} \times (1-0.9)} \simeq 18,118.$$

Fig. 5(a) and (b) shows $q_{z_{max}}$ and $V_{z_{max}}$ as a function of k in a QIT defined for first stability region when $0 \leq k < 1$, respectively. To plot Fig. 5(a) and (b) we used extended of Tables 2 and 3 when $k = 0$ up to 0.9 using 0.1 steps. Fig. 5(a) shows that with increasing k from 0 to 1, $q_{z_{max}}$ decrease and Fig. 5(b) shows that with increasing it k from 0 to 1, $V_{z_{max}}$ increase also. The higher V_{rf} will have the better mass separations especially, for the lower ion mass range.

5. Ion trajectories

Figs. 6 and 7 show the ion trajectories in real time and $r-z$ plan for $\beta_z = 0.99$, respectively, black line: $k = 0$ and blue line: $k = 0.9$. Fig. 8 shows the evolution of the phase space ion trajectory for different values of the phase τ_0 for $\beta_z = 0.99$, line: $k = 0$, dot line: $k = 0.9$, (a) $z - \dot{z}$ plan and (b) $r - \dot{r}$ plan. Fig. 9 shows the stability diagram in (U, V) for $k = 0\,; 0.9$ and (a) $m = 1$ amu, (b) $m = 2$ amu.

6. Discussion and conclusion

The results of the numerical integration of the Mathieu equation with the help of the fifth-order Runge–Kutta method showed that, the apex of the stability parameters a_z stayed the same. For example, the third stability regions has $a_z \leq 8.683$ for $k = 0$ and $k = 0.9$. But, the stability parameter $q_{z_{max}}$ substantially decreases for higher k values. In practice, this situation might bring certain problems for impusional potential because, higher harmonics have to be amplitude. However, as long as the amplitude of the harmonic components stays fairly constant, there will be no problems.

The mechanical properties of an ion under both excitation potentials; $k = 0$ and $k = 0.9$, were compared using the ion displacements such as; the real time, $r - z$ plane and phase space. As far as first stability concern, and for the same β_z points (see Figs. 6–8), no difference found in the ion behaviors.

From the results, it is seen that, a reduction in the first stability diagrams in the a_z, q_z plane (see Fig. 3) will resulted in the higher V_{rf} voltage values (see Figs. 5(b) and 9).

As an example, consider the following QIT operational parameters with *rf* only mode; $U = 0$ ($a_z = 0$), $\Omega = 2\Pi \times 1.05 \times 10^6$ rad s^{-1}, $z_0 = 0.783$ cm. The values V_{rf} voltage (correspond to the $q_{z_{max}}$) for ^{131}Xe ion is $V_{rf} = 1812$ V for $k = 0$ and $V_{rf} = 18,118$ V for $k = 0.9$. Moreover, with the same operational parameters, the separation voltages ΔV_{rf} for mass range of 1–2 amu (hydrogen and hydrogen like isotopes) ions are $\Delta V_{rf} = 11$ V for $k = 0$ and $\Delta V_{rf} = 130$ V for $k = 0.9$ (see Fig. 9). This indicates that, there is about 12 times more confining voltage needed for the impusional voltage compared to the classical sinusoidal case for the same ion mass-to-charge ratio. The higher ΔV_{rf} the better mass separations especially, for the lower ion mass range; the amplification of the higher order harmonics in the impulsional voltage without any distortion. Also, if the impulsional voltage ejection phase is fixed for a maximum, e.g. $\cos(\Omega t) = 1$, higher potential energy will be available for ions to get out of QIT, and eventually less ion desperation's.

References

[1] R.E. March, J.F.J. Todd, Practical Aspects of Ion Trap Mass Spectrometry, CRC Press, New York, 1995.
[2] R.E. March, J. Mass Spectrom. 32 (1997) 263.
[3] J. Martin-Vaquero, B. Janssen, Comput. Phys. Commun. 180 (2009) 1802.
[4] N.W. McLachlan, Theory and Application of Mathieu Functions, Clarendon, Oxford, 1947.
[5] W. Paul, H. Steinwedel, Z. Naturforsch. A 8 (1953) 448.
[6] D.J. Wineland, W.M. Itano, J.C. Bergquist, Opt. Lett. 12 (1987) 389.

[7] W.M. Itano, J.C. Bergquist, R.G. Hulet, D.J. Wineland, Phys. Rev. Lett. 59 (1987) 2732.
[8] W.M. Itano, D.J. Heinzen, J.J. Bollinger, D.J. Wineland, Phys. Rev. A 41 (1990) 2295.
[9] J. von Zanther, J. Abel, Th. Becker, M. Fries, E. Peik, H. Walther, R. Holzwarth, J. Reichert, Th. Udem, T.W. Hansch, A.Yu. Nevsky, M.N. Skvortsov, S.N. Bagayev, Opt. Commun. 166 (1999) 57.
[10] R.J. Rafac, B.C. Young, J.A. Beall, W.M. Itano, D.J. Wineland, J.C. Berquist, Phys. Rev. Lett. 85 (2000) 2462.
[11] F. Kashanian, S. Nouri, S. Seddighi Chaharborj, A.B. Mohd Rizam, Int. J. Mass Spectrom. 303 (2011) 199.
[12] D. Kielpinski, V. Meyer, M.A. Rowe, C.A. Sackett, W.M. Itano, C. Monroe, D.J. Wineland, Science 291 (2001) 1013.
[13] A. Steane, C.F. Roos, D. Stevens, A. Mundt, D. Leibfried, F. Schmidt-Kaler, R. Blatt, Phys. Rev. A 62 (2000) 042305.
[14] S.M. Sadat Kiai, A.R. Zirak, M. Elahi, S. Adlparvar, B.N. Mortazavi, A. Safarien, S. Farhangi, S. Sheibani, S. Alhooie, M.M.A. Khalaj, A.A. Dabirzadeh, M. Ruzbehani, F. Zahedi, J. Fusion Energy, doi:10.1007/s10894-010-9296-9.
[15] S.M. Sadat Kiai, J. Andre, Y. Zerega, G. Brincourt, R. Catella, Int. J. Mass Spectrom. Ion Process. 107 (1991) 191–203.
[16] S.M. Sadat Kiai, Y. Zerega, G. Brincourt, R. Catella, J. Andre, Int. J. Mass Spectrom. Ion Process. 105 (1991) 65.
[17] S.M. Sadat Kiai, Int. J. Mass Spectrom. 188 (1999) 177.
[18] S.M. Sadat Kiai, M. Baradaran, S. Adlparvar, M.M.A. Khalaj, A. Doroudi, S. Nouri, A.A. Shojai, M. Abdollahzadeh, F. Abbasi, D.M.V. Roshan, A.R. Babazadeh, Int. J. Mass Spectrom. 247 (2005) 61–66.
[19] S. Seddighi Chaharborj, S.M. Sadat Kiai, J. Mass Spectrom. 45 (2010) 1111.
[20] N. Yaacob, D.J. Evans, Int. J. Comput. Math. 65 (1997) 141.
[21] M.N. Benilan, C. Audoin, Int. J. Mass Spectrom. 11 (1973) 421.